Basic Bifurcation Phenomena

WOB — Tutorial 2

R. Seydel

World of Bifurcation

Version June 1999

Universität Köln
Mathematisches Institut
Weyertal 86-90
D-50931 Köln

Tel.: +49(0)221 470 4335
FAX: +49(0)221 470 4340
e-mail: seydel@mi.uni-koeln.de

The models that describe our nonlinear phenomeana are defined through the language of mathematics. The equations representing the models may be ordinary differential equations (ODEs), or partial differential equations (PDEs). Moreover, some problems are described by "algebraic" equations, or by integral equations, or by some mixture. In addition to the differential equations there may be boundary conditions or initial conditions. Faced with the great variety of possible combinations and formats we basically restrict ourselves to the ODE situation. Many of the ideas and methods can be applied in a similar way to other equations.

1. A computer experiment

We define $y_1(t)$ and $y_2(t)$ to be functions that solve the system of two ODEs

$$\begin{aligned} \dot{y}_1 &= -y_1 + \lambda(1 - y_1)\exp(y_2) \\ \dot{y}_2 &= -y_2 + 16.2\lambda(1 - y_1)\exp(y_2) - 3y_2 \end{aligned}$$

and satisfy the initial values

$$y_1(0) = 0.5, \quad y_2(0) = 0.5;$$

for the background see WOBexd2. The symbol λ stands for a parameter that may take values in a range, say, between 0.125 and 0.26. Take any code for integrating ODE initial-value problems, and integrate the equations for the time interval $0 \le t \le 30$.

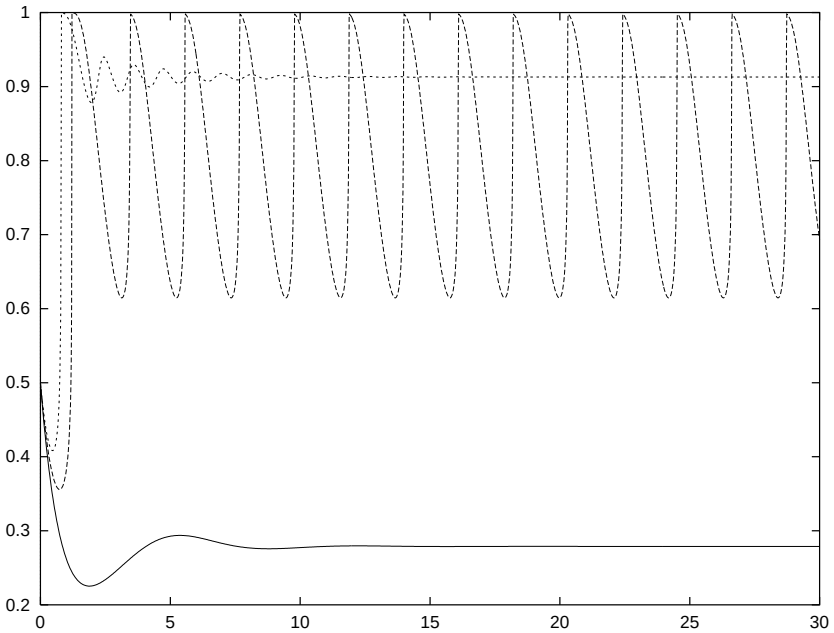

Fig. 1. Computer experiment. vertical axis: y_1, horizontal axis: time t. curves: behavior of $y_2(t)$ for three values of the parameter λ: 0.125 (solid line), 0.2 (dashed), 0.26 (dotted).

For the first series of experiments we take constant values of λ for each integration, but vary λ from one integration to the next. This treatment of the parameter λ as being constant but variable is called *quasistationary* variation. In Figure 1 we observe the results for three selected values of λ, namely $\lambda = 0.125$, $\lambda = 0.2$, and $\lambda = 0.26$. For example, take $\lambda = 0.125$: We observe that after a **transient phase** of, say, $0 \leq t \leq 10$, the trajectory $y_1(t)$ becomes stationary — that is, it is attracted by a state with a constant value. For $\lambda = 0.2$ there is again a transient phase, after which the trajectory becomes periodic with large oscillations. The stationary state, and the periodic state respectively attract the neighboring trajectory. Both attracting states are regular in shape. Finally, for $\lambda = 0.26$ the attractor is again stationary, but now on a higher level. The experiment has shown that the level and the quality of solutions *vary with the parameter*.

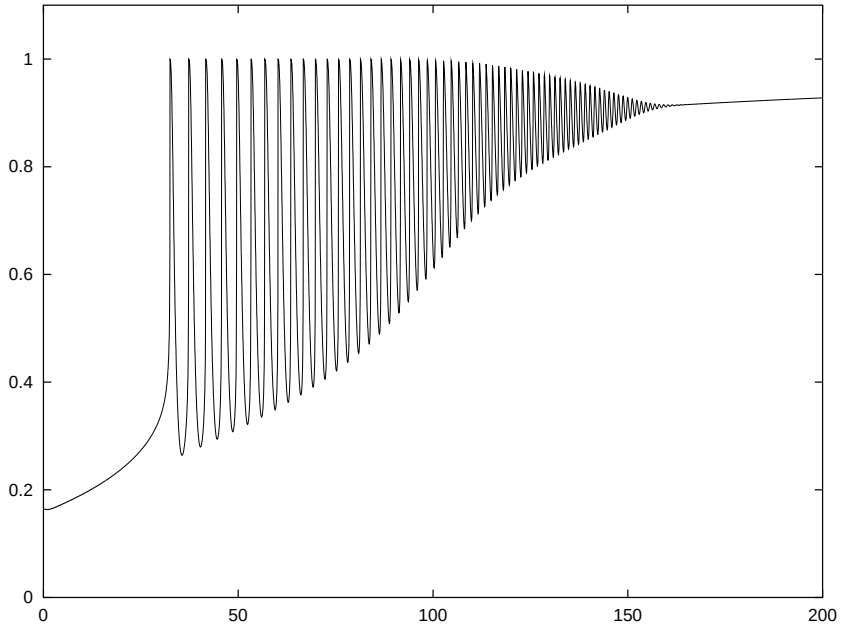

Fig. 2. $y_1(t)$ for $0 \leq t \leq 200$ and λ varying from 0.1 to 0.3

In a second type of experiment we let the parameter drift slowly in a nonstationary way, $\dot{\lambda} \neq 0$. In order to move with the parameter through a range that matches the first set of experiments, we chose the additional differential equation

$$\dot{\lambda} = 0.001, \quad \lambda(0) = 0.1$$

We may denote $y_3 := \lambda$ and integrate a coupled system of three ODEs for $0 \leq t \leq 200$. The result is seen in Figure 2. Because of the linear variation of λ, the horizontal axis can be exchanged by an equivalent λ-axis extending from $\lambda = 0.1$ to $\lambda = 0.3$, which would indicate the current value of the parameter. Observing the result of Figure 2, we come closer to an explanation of our quasistationary treatment reported above. There appears to be a sudden transition from a more or less stationary state to a strongly oscillating state at $t \approx 40$ ($\lambda \approx 0.14$). For further increasing t (or λ) the

amplitude of the oscillation dimishes and dies out for $t \approx 150$ ($\lambda \approx 0.25$). Since λ is not constant, the experiment reported in Figure 2 does not settle in to a purely stationary or purely periodic state. We note that for drifting parameters the location of the attractor varies continuously, and the trajectory follows. Summarizing this experiment we note that for $\lambda \approx 0.14$ and $\lambda \approx 0.25$ a **threshold** of the parameter is passed. Later we shall explain such thresholds and the mechanism of switching attractors as *bifurcations*.

2. The model problem

We assume that our biological, physical, technical ... problem is modelled by the first-order system of ODEs

$$\dot{\mathbf{y}} = \mathbf{f}(\mathbf{y}, \lambda) \tag{1}$$

where $\mathbf{y}(t)$ is a vector function with n components $y_i(t)$, $i = 1, \ldots, n$. The overdot indicates differentiation with respect to time t, and $\mathbf{f}$ is the *right-hand side* defining the dynamical law. The state $\mathbf{y}$ that solves Eq.(1) depends on the real parameter $\lambda \in \mathbb{R}$. **Stationary solutions** $\mathbf{y}^s$ of (1) solve

$$\mathbf{f}(\mathbf{y}^s, \lambda) = \mathbf{0}. \tag{2}$$

Periodic solutions of the autonomous system (1) satisfy $\mathbf{y}(t + T) = \mathbf{y}(t)$ for all t and a minimum period $T > 0$.

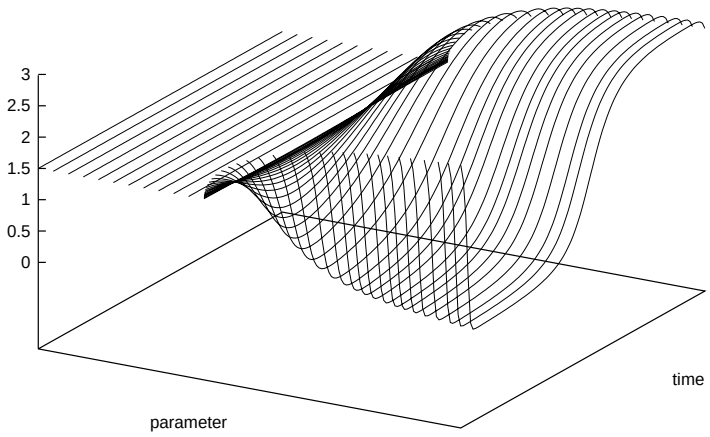

Fig. 3. Stable solutions of Eq.(3), $y_1(t; \lambda)$ for $0.2 \leq \lambda \leq 3$.

3. An example from chemistry

As an example consider WOBexd6, a chemical reaction with autocatalytic step

$$\begin{aligned} \dot{y}_1 &= 3 - y_1 - \lambda y_1 y_3, \\ \dot{y}_2 &= y_1 - y_2 y_3, \\ \dot{y}_3 &= y_2 y_3 - \lambda y_1 y_3, \end{aligned} \tag{3}$$

which is taken from [Krug & Kuhnert, 1985]. Equation (3) is of the format of Eq.(1), with $n = 3$. In Figure 3 we show solutions that are *stable*—that is, the impact of small perturbations of the solutions decays to zero. Solutions $\mathbf{y}$ depend on time t, and on the parameter λ. Both dependencies are indicated in Figure 3 where we show solution profiles $y_1(t;\lambda)$ for various discrete values of the parameter λ out of the interval $0.2 \le \lambda \le 3$. There is a critical parameter value $\lambda_0 = 1.30176$ separating two different regimes. For $\lambda < \lambda_0$ the stable solution is stationary. Each solution profile in that regime is constant. The situation is different for $\lambda > \lambda_0$ where the calculated stable solutions are periodic. As can be seen in Figure 3, the amplitudes of the periodic orbits grow from zero (at λ_0) to larger values when λ is increased. The period varies too; the initial period for λ_0 is $T_0 = 6.035555$. The figure depicts the values of $y_1(t)$ for one period; the periods are scaled to unity. The two other components y_2, and y_3 vary similarly. Figure 3 depicts the asymptotic situation with attracting stationary and periodic states; transient initial phases are not shown. The stability of the solutions is indicated by the phase diagrams of Figure 4, and Figure 5. Since the trajectories $\mathbf{y}(t)$ of Eq.(3) are in the three-dimensional phase space $\mathbb{R}^3$ we have projected the curves in space to a plane for easy graphical demonstration. Here the projection is to the (y_1, y_2)-plane. Starting from $\mathbf{y}(0) = (2, 1, 1)$ we show the transient initial phase where the trajectory approaches the "next" attractor. Figure 4 (for $\lambda = 1$) depicts a situation with a stable spiral, and Figure 5 ($\lambda = 1.5$) shows a projection of the dynamics of an attracting periodic orbit. Note that the trajectories do not intersect in the reality of phase space $\mathbb{R}^n$. As Figure 3 shows, periodic solutions are born at λ_0; this phenomenon is called **Hopf bifurcation**.

Looking back at Figure 2 we may notice that the phenomenon taking place for $t \approx 150$ ($\lambda \approx 0.25$) is of that kind. Here, in the quasistationary setting of Eq.(3), the attractors come out most regularly, as in Figure 3.

4. Branches

As illustrated by the above example of Eq.(3), and by the computer experiment of section 1, solutions in general vary when the parameter is changed. Figure 3 has shown solutions for a discrete selection of λ values. We could have chosen any intermediate value of λ and would have obtained solutions between those depicted. There is a *continuum* of solutions parameterized by λ. The slices in Figure 3 extend to a continuous surface. We call a smooth continuum of solutions a **branch**.

The implicit function theorem (see any textbook of analysis) specifies sufficient criteria guaranteeing that a branch can be parameterized by λ. For a specific stationary solution $(\mathbf{y}^{\lambda_1}, \lambda_1)$ of Eq.(2) the criterion basically requires nonsingularity of the

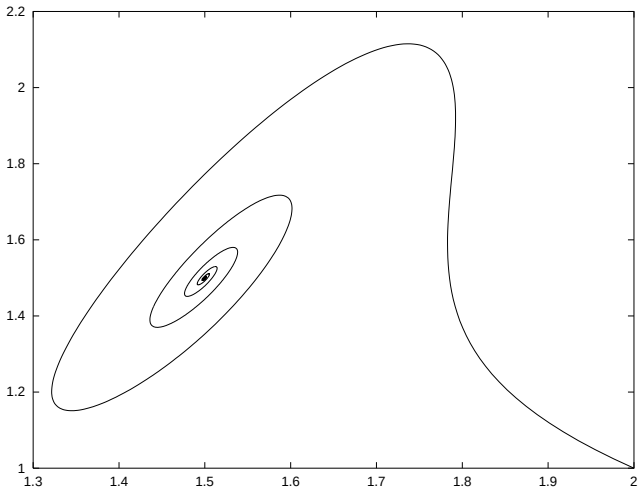

Fig. 4. Eq.(3), $\lambda = 1$, projection to the (y_1, y_2) plane.

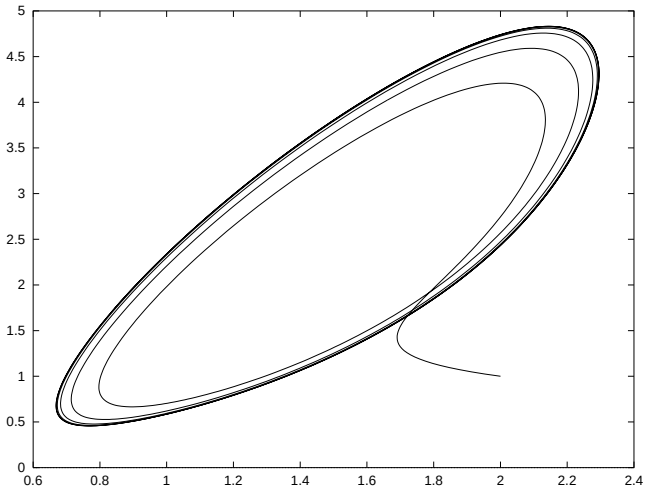

Fig. 5. Eq.(3), $\lambda = 1.5$, projection to the (y_1, y_2) plane.

Jacobian matrix $\mathbf{f_y}(\mathbf{y}^{\lambda_1}, \lambda_1)$. Then there is an interval around λ_1 such that for all λ in that interval Eq.(2) has a solution $\mathbf{y}^\lambda$ close to $\mathbf{y}^{\lambda_1}$.

5. An example from electrical engineering

The trigger circuit from WOBexa2 is described by

$$\begin{aligned}
f_1 &= (y_1 - y_3)/10000 + (y_1 - y_2)/39 + (y_1 + \lambda)/51 = 0,\\
f_2 &= (y_2 - y_6)/10 + I(y_2) + (y_2 - y_1)/39 = 0,\\
f_3 &= (y_3 - y_1)/10000 + (y_3 - y_4)/25.5 = 0,\\
f_4 &= (y_4 - y_3)/25.5 + y_4/0.62 + y_4 - y_5 = 0,\\
f_5 &= (y_5 - y_6)/13 + y_5 - y_4 + I(y_5) = 0,\\
f_6 &= (y_6 - y_2)/10 - [U_{\mathrm{A}}(y_3 - y_1) - y_6]/0.201 + (y_6 - y_5)/13 = 0;
\end{aligned} \tag{4}$$

$$U_{\mathrm{A}}(U) = 7.65 \ \arctan\,(1962U), \quad I(U) = 5.6 \cdot 10^{-8}(e^{25U} - 1).$$

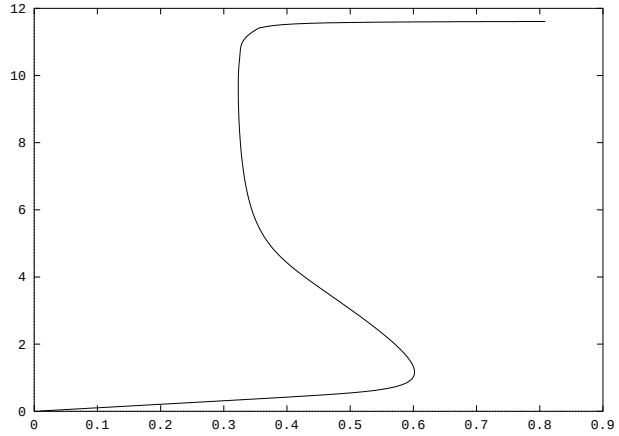

Fig. 6. Trigger Eq.(4), output voltage y_6 versus input voltage λ.

This problem from [Pönisch & Schwetlick, 1982] is of the form $\mathbf{f}(\mathbf{y}, \lambda) = \mathbf{0}$, with $n = 6$. The variables y_i are voltages. The input voltage is λ, the output voltage is y_6. Solving Eq.(4) yields the hysteresis-type response diagram in Figure 6. Diagrams like Figure 6 depicting a scalar representative of $\mathbf{y}$ versus the parameter λ are called **branching diagram**, or **bifurcation diagram**, or **response diagram**. (We use "bifurcation" and "branching" as synonyms.) The branch of solutions is a (one-dimensional) curve in the seven-dimensional $(\mathbf{y}, \lambda)$-space. The curve in Figure 6 is a projection to the (y_6, λ)-plane. The bistable situation of the trigger is characterized by two bounding critical solutions where the branch can not be parameterized by λ; the tangent to the branch in these points is "vertical" (i.e., perpendicular to the λ-axis). These two *turning points* have the threshold values $\lambda_0 = 0.601853$, and $\lambda_0 = 0.322866$. Obviously these are thresholds where jumps to the other stable level take place. At these critical solutions the Jacobian $\mathbf{f_y}$ is singular. But note that the curve can be parameterized by y_6. A turning point is also called **fold bifurcation**, or *saddle node*.

Fold bifurcations are frequently occurring in applications. For a boundary value problem (not of the type of Eq.(1)) see the Duffing oscillator WOBexb3, or the catalytic reaction WOBexb1, or the electric power system WOBexd15.

6. Bifurcation

Loosely speaking, a *bifurcation with respect to* λ is a specific solution at λ_0 where there is no neighborhood around λ_0 such that in this neighborhood the branch can be uniquely extended. In short, at a bifurcation something "happens." Qualitative changes are tied to bifurcations. We have seen examples: The two turning points in the trigger problem (see Figure 6) are bifurcation points. The Hopf bifurcation point of the example of Eq.(3) is another example, which needs more explanation. Schematically, the Hopf situation is as illustrated in the branching diagram of Figure 7a.

At a Hopf bifurcation, the branch of stationary solutions does not bifurcate; the Jacobian matrix $\mathbf{f_y}(\mathbf{y}_0, \lambda_0)$ is nonsingular. In Figure 7a, the branch of stationary

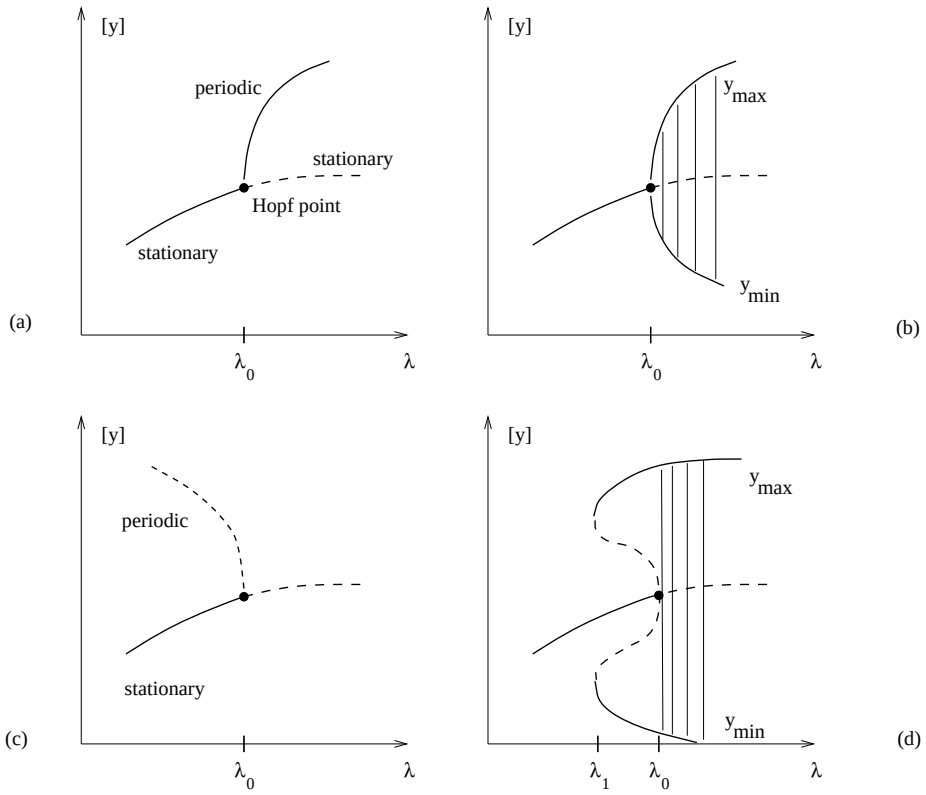

Fig. 7. Hopf scenarios.

solutions extends beyond λ_0, but it is unstable for $\lambda > \lambda_0$. The Jacobian at a Hopf bifurcation has a pair of purely imaginary eigenvalues $\pm i\beta$. Here a branch of periodic orbits is born. In Figure 7a, for $\lambda > \lambda_0$, $\lambda \to \lambda_0$ the periodic solutions merge into the stationary branch, the amplitude vanishes. The bifurcation is vertical, and the amplitude locally behaves like $\sqrt{|\lambda - \lambda_0|}$. This is seen in Figure 3, just concentrate on the y_1-values belonging to the minimum t-value. The vertical axes in Figure 7 depict a scalar measure of the solutions, such as

$$[\mathbf{y}] = y_1(t^*) \quad \text{where } \dot{y}_1(t^*) = 0.$$

That is, $[\mathbf{y}]$ depicts a relative maximum, or minimum of y_1. With this illustration, the periodic oscillation can be visualized as in Figure 7b.

The situation of Figures 7a, 7b depicts a transition without jump: Passing λ_0 when increasing λ one experiences a *soft loss* of stability of the stationary state; the bifurcation is *supercritical*. In Figure 7c we illustrate a *subcritical* situation where locally no stable state exists on one side of λ_0 (here for $\lambda > \lambda_0$). Globally, this local scenario of Figure 7c often extends to a different situation, see Figure 7d: The branch of unstable periodic orbits bends back, gaining stability at a turning point like situation. Consequently, when we increase λ beyond the critical Hopf parameter value λ_0 a jump occurs. For $\lambda > \lambda_0$ in Figure 7d, there are no neighboring small-amplitude periodic solutions, and the dynamics is immediately attracted by a large-amplitude oscillation. This large jump is the *hard loss* of stability. Note that Figure 7d shows

a bistable situation for $\lambda_1 < \lambda < \lambda_0$. Note further that the described scenarios may also happen for *de*creasing λ.

Examples for a hard loss of stability are the computer experiment (WOBexd2), the bogie model (WOBexd10), the nerve model WOBexd14, and the power system WOBexd15. Examples for a soft loss of stability are again the computer experiment (the "right" bifurcation), the Brusselator (WOBexd1), and the reaction of Eq.(3).

In any arbitrary example of the type of Eq.(1) one must expect the occurrence of a fold bifurcation, or of a Hopf bifurcation. There are other bifurcations which are less likely to be found in a general equation. But many equations involve some symmetry. Often the symmetry in the equations reflects the common situation that a model consists of two or more identical parts that are coupled. When two identical subsystems are suitably coupled, one can exchange their states by a simple reflection. The related symmetry is the Z_2-symmetry. For equations with a Z_2-symmetry the **pitchfork bifurcation** is common too.

For a Z_2-pitchfork bifurcation, the emanating branch consists of solutions that lose their symmetry. This phenomenon is called **symmetry breaking**. Schematically, the related bifurcation diagrams resemble those of Figure 7 of the Hopf scenario; compare Figure 8. The two asymmetric half-branches can be identified because they are transformed into each other by the underlying reflection that describes the exchange of the states of the subsystem.

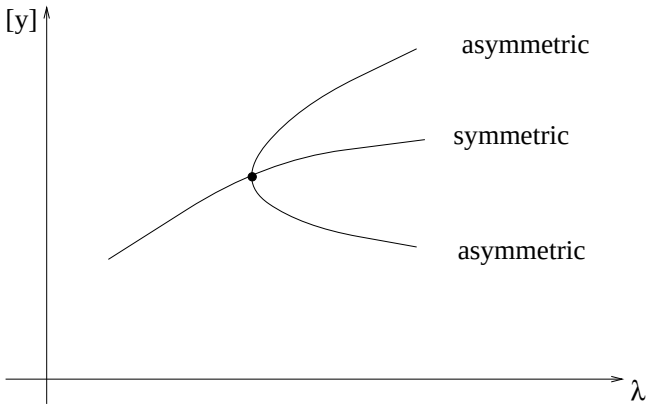

Fig. 8. Z_2-Pitchfork Scenario.

Examples of such pitchfork bifurcations are the Brusselator reaction WOBexa1, the flipflop WOBexa11, WOBexd1, the superconductivity WOBexb2, and the Duffing oscillator WOBexb3.

7. Period doubling and chaos

So far we have assumed solutions to Eq.(1) being regular in the sense *stationary*, or *periodic*. The deterministic system (1) allows for aperiodic solutions that have been named *chaotic*. There are several ways how to explain the onset of chaos. One of the most suggestive scenarios of chaos is tied to *period doubling*.

The local stability of a periodic orbit $\mathbf{y}$ is determined by the eigenvalues of the monodromy matrix $\mathbf{M} := \Phi(T)$ where $\Phi(t)$ is the matrix function that solves the linear matrix initial-value problem

$$\dot{\Phi} = \mathbf{f}_{\mathbf{y}}(\mathbf{y}, \lambda)\Phi, \quad \Phi(0) = \mathbf{I}. \tag{5}$$

These eigenvalues of $\mathbf{M}$ are called *multipliers*. One of the n eigenvalues is always unity, $\mu_n = 1$. The other $n-1$ multipliers $\mu_1, \ldots, \mu_{n-1}$ are monitored to examine whether they are inside the unit circle ($|\mu| < 1$), or outside. The periodic orbit is locally stable in the case when all $n-1$ multipliers are inside the unit circle. Also the eigenvalues depend on the parameter, $\mu = \mu(\lambda)$. Varying λ can result in one or more multipliers crossing the unit circle. Assume this happens for λ_0, $|\mu_j(\lambda_0)| = 1$ for some j. Then the solution corresponding to λ_0 is a bifurcation. Different types of bifurcation occur depending on where $\mu_j(\lambda)$ crosses the unit circle. The period doubling happens in the case $\mu_j(\lambda_0) = -1$.

Dynamically, the period doubling bifurcation (or **flip bifurcation**) is the following scenario: Assume a branch of periodic solutions parameterized by λ with stable orbits on one side of λ_0 (say, $\lambda < \lambda_0$) and a multiplier crossing the unit circle with $\mu(\lambda_0) = -1$. Then, locally, there are periodic orbits with the double period near λ_0. These double-periodic orbits form a new branch that emerges at λ_0. Note that the periods vary with λ, and the factor 2 of period doubling holds only asymptotically for $\lambda \to \lambda_0$. The situation typically is as in the left part of Figure 9, for $\lambda_0 = \lambda_{01}$.

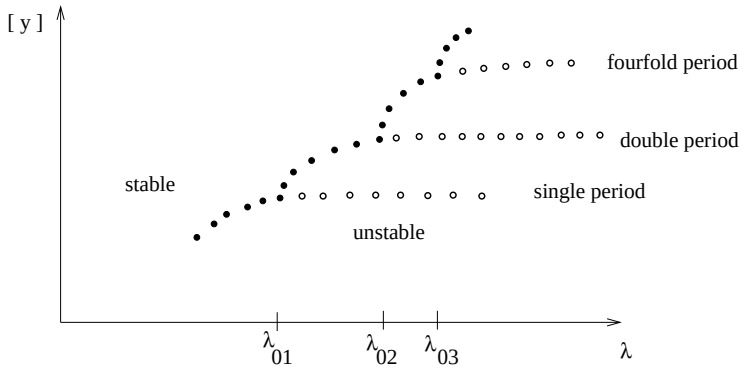

Fig. 9. Cascade of period doublings, schematically.

The "new" branch with the "double" period can experience a period doubling, too (in Figure 9, for λ_{02}). There are many important applications were an infinite chain of such period doublings occurs for λ_{01}, λ_{02}, λ_{03}, ... In the supercritical case, the stability is exchanged to the branches of the double period. After some period doublings the period has become so large that the orbit looks irregular. As has been shown, the bifurcation values $\lambda_{0\nu}$ satisfy a universal scaling law,

$$\lim_{\nu \to \infty} \frac{\lambda_{\nu+1} - \lambda_\nu}{\lambda_\nu - \lambda_{\nu-1}} = 0.214169\ldots \tag{6}$$

This scaling law, named after Feigenbaum, has a remarkable consequence: There is an accumulation point λ_∞ of the sequence of period doubling bifurcations. Passing λ_∞

means that the "period" has reached infinity. The resulting solution is fully aperiodic, and is "chaotic." In this scenario the irregularity of a chaotic solution can be explained by the infinite number of unstable periodic orbits (UPOs) that are "left behind" at the infinite sequence of period doublings. Imagine the **y** state space is packed with UPOs, all repelling any trajectory that searches a path through that area. This state of continuously being pushed by UPOs may explain the sensitive dependence on the initial conditions that is a characterisitic criterion of chaos.

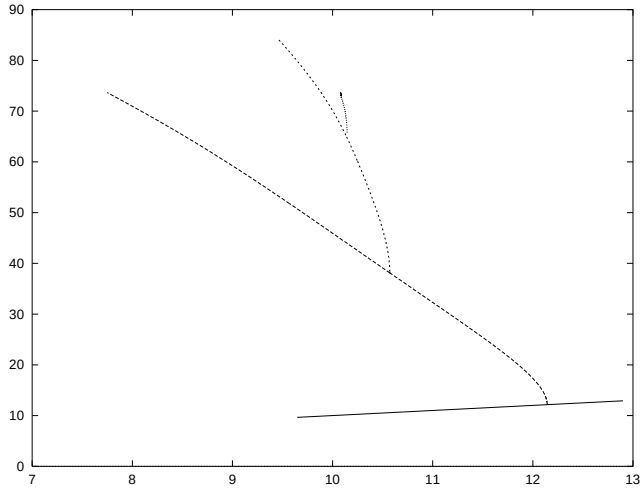

Fig. 10. Eq.(7), bifurcation diagram $y_1(0)$ versus λ.

8. An example: isothermal reaction

An isothermal reaction (from [Smith *et al.*, 1983], WOBexd13) is modelled by

$$\begin{aligned} \dot{y}_1 &= y_1(30 - 0.25y_1 - y_2 - y_3) + 0.001y_2^2 + 0.1, \\ \dot{y}_2 &= y_2(y_1 - 0.001y_2 - \lambda) + 0.1, \\ \dot{y}_3 &= y_3(16.5 - y_1 - 0.5y_3) + 0.1 \ . \end{aligned} \tag{7}$$

There is a Hopf bifurcation at $\lambda_0 = 12.1435$, and a sequence of period doubling bifurcations, compare the branching diagram Figure 10. The critical parameter values of period doubling are

$$\begin{aligned} \lambda_1 &= 10.5710 \\ \lambda_2 &= 10.1465 \\ \lambda_3 &= 10.0912 \\ \lambda_4 &= 10.0808. \end{aligned}$$

These four values allow to calculate two of the Feigenbaum ratios in Eq.(6). The ratios are 0.13, and 0.19. The asymptotic law allows to estimate the accumulation point where chaos sets in. From Eq.(6) we derive the estimate

$$\lambda_\infty = \frac{\delta\lambda_{\nu+1} - \lambda_\nu}{\delta - 1} \qquad \text{for } \delta = 4.6692016 \tag{8}$$

Applying this to our sequence of period doublings we estimate that λ_∞ is as close as $\lambda_\infty \approx 10.078$. Figures 11a, 11b show phase portraits of a periodic orbit of the "double" period for $\lambda = 10.55$, and of the fourfold period ($\lambda = 10.13$). Figure 12 depicts an apparently chaotic solution for $\lambda = 10$. The sequence of bifurcations from stationary state ($\lambda = 12.9$) to "period four" ($\lambda = 10.1$) is illustrated by Figure 13. Another interesting example with period doublings is the voltage collapse problem WOBexd15.

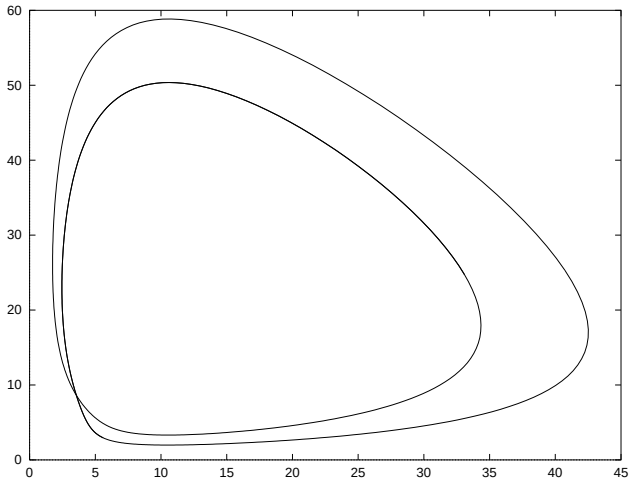

Fig. 11a. Eq.(7), periodic orbit, $\lambda = 10.55$, projection to (y_1, y_2) plane.

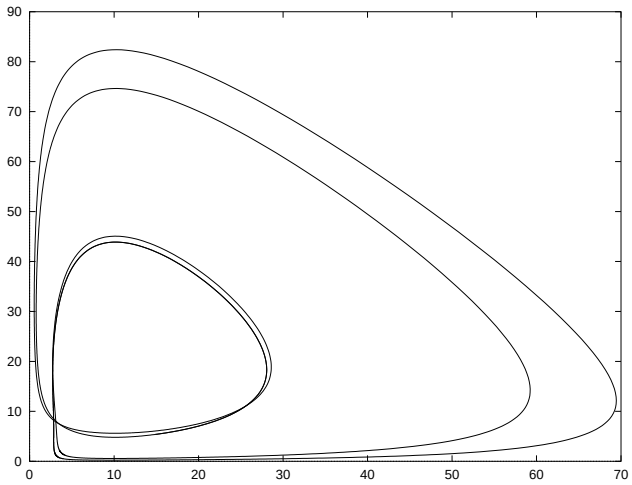

Fig.11b. Eq.(7), periodic orbit, $\lambda = 10.13$, projection to (y_1, y_2) plane.

9. Other bifurcations

So far we have introduced three bifurcation mechanisms, namely turning point (fold bifurcation), Hopf bifurcation, and period doubling (flip bifurcation). These three bifurcations are the most important ones for a problem of the type of Eq.(1), because they occur most frequently in applications. There are other bifurcation phenomena which we briefly list.

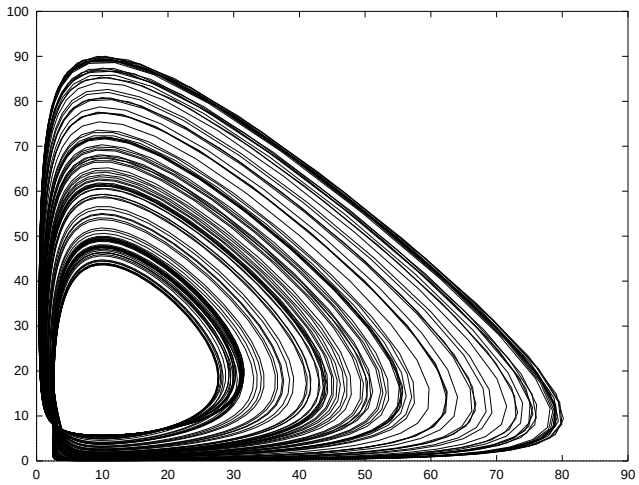

Fig. 12. Eq.(7), chaotic orbit, $\lambda = 10$, projection to (y_1, y_2) plane.

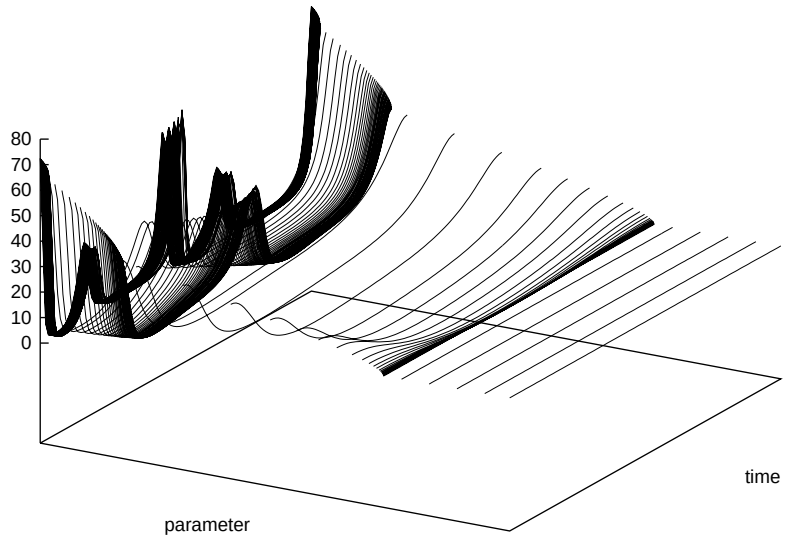

Fig. 13. Eq.(7), $y_1(t;\lambda)$ for $10.1 \leq \lambda \leq 12.9$, periods scaled to unity.

First we return to the pitchfork. The simplest equation with pitchfork is $0 = \lambda y \pm y^3$. The simplest equations exhibiting a certain phenomenon are called *normal forms*. As mentioned above, in case the underlying equation supports a Z_2-symmetry, the pitchfork scenario is also likely to occur. The geometrical analogy of a pitchfork illustration with that of a Hopf bifurcation is no coincidence since the normal form of Hopf bifurcation is (in polar coordinates ρ, ϑ)

$$\begin{aligned} \dot{\rho} &= \lambda\rho - \rho^3 \\ \dot{\vartheta} &= 1. \end{aligned} \tag{9}$$

Solutions of this normal form include the stationary state $\rho \equiv 0$, and the periodic

state $\rho(t) \equiv \sqrt{\lambda}$. In both cases $\dot{\rho} = 0$ holds, and we have a pitchfork characterization of the amplitude. If the equation supports no symmetry, then to have a pitchfork more parameters than just λ are required. Classifications of related bifurcations of higher *codimension* can be found in [Golubitsky & Schaeffer, 1985]. The higher the codimension, the less likely it is to find one. But bifurcations of higher codimension play a prominent role as organizing centers in parameter space. We shall briefly return to this in Section 10.

Branches of periodic orbits can show more bifurcation phenomena than just period doubling. The multipliers can cross the unit circle of the complex plane at $+1$. Then we encounter, for example, a turning point, or a pitchfork bifurcation. The turning point of periodic orbits is sometimes called **cyclic fold bifurcation**. When the crossing is with nonzero imaginary part, there is a bifurcation into a torus-like object.

Periodic orbits are born in a Hopf bifurcation, and may end in a **homoclinic orbit**. To explain the simplest such scenario imagine in a plane a stationary state of saddle type. This saddle has a pair of entering trajectories and a pair of leaving trajectories. In case the leaving trajectory bends back such that it is identical with the entering trajectory we have a loop with infinite period. This is a homoclinic orbit. A periodic stable orbit close to a saddle is depicted in the phase portrait of Figure 14. Assume this is the situation for $\lambda = \lambda_0 + \epsilon$, and the periodic orbit and the saddle approach each other for $\epsilon \to 0$. Then we encounter a homoclinic orbit for λ_0 and no periodic orbit for $\lambda_0 - \epsilon$.

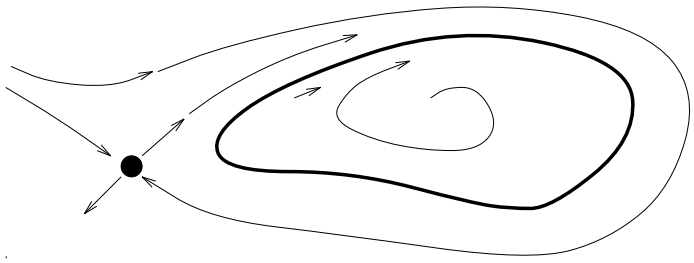

Fig. 14. Situation close to a homoclinic orbit.

This simplest scenario of a homoclinic orbit illustrates how an unstable stationary state annihilates a periodic orbit. Analog phenomena are also possible with other unstable states. For example, a collision of an unstable periodic orbit might terminate a chaotic attractor. Generally, unstable states play a fundamental role in organizing dynamical behavior. This situation stresses the importance of calculating also unstable states. An example of the decisive role an unstable state plays in "killing" the operating regime is provided by models of voltage collapse, see WOBexd15.

10. Multi-parameter problems

The problems discussed so far depend on one real parameter λ. The standard situation in applications is that problems have several parameters λ, γ, δ, ..., say, m

parameters. In freezing $m-1$ parameters to fixed values, and varying only one parameter (say, λ), all the bifurcation phenomena mentioned above may occur. If we unfreeze a second parameter (say, γ), all bifurcation results depend on γ. In particular, the critical bifurcation values λ_0 vary with γ. In the (λ, γ)-parameter plane the loci of bifurcations are *curves*, the *bifurcation curves*. Specifically, the Hopf bifurcations constitute the **Hopf curves**, and the turning points form the **fold curves**. The points (λ_0, γ_0) where such bifurcation curves meet in the parameter plane are bifurcations of higher singularity.

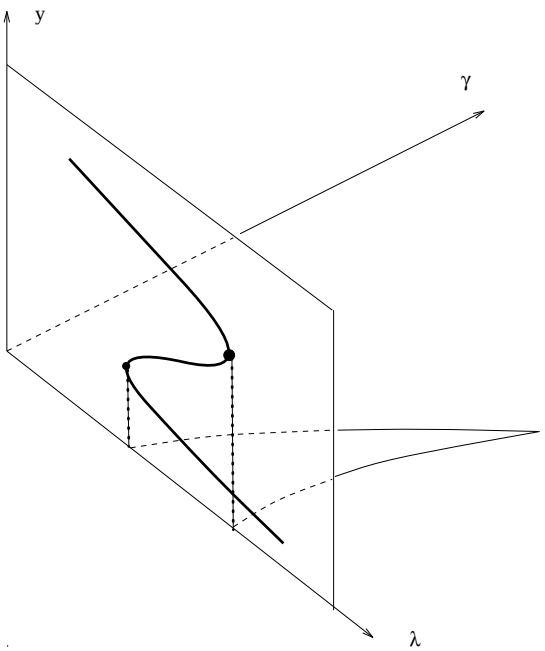

Fig. 15. Cusp scenario, with fold curves.

As a simple example, imagine a hysteresis situation as depicted in Figure 6. The range of bistability between the values λ_0 of the two turning points may shrink when a second parameter γ is varied, see Figure 15. Denote γ_0 the specific value where both λ_0-values coincide. Then, on one side of γ_0 (say for $\gamma < \gamma_0$) a bistable situation with jump phenomena exists whereas on the other side no bistability, and no bifurcation of that kind exists. Exactly for $\gamma = \gamma_0$ the bifurcation is a *hysteresis point*, the two adjacent turning points have collapsed into a point of inflection. The value γ_0 is seen as an *organizing center* separating two completely different dynamical situations. This is illustrated by the parameter chart of Figure 16. The figure depicts also a jump-free transition from one operation point in the parameter plane to another. A related example is provided by a catalytic reaction (WOBexb1). The knowledge of the bifurcation curves allows to find easily a curve of parameter combinations (λ, γ) that detours and avoids the jumps triggered by turning points.

If in addition to λ and γ, a third parameter is considered to be freely variable, the bifurcation curves in the parameter plane extend to *bifurcation surfaces* in the parameter space. Possible bifurcation scenarios become even more involved. A the-

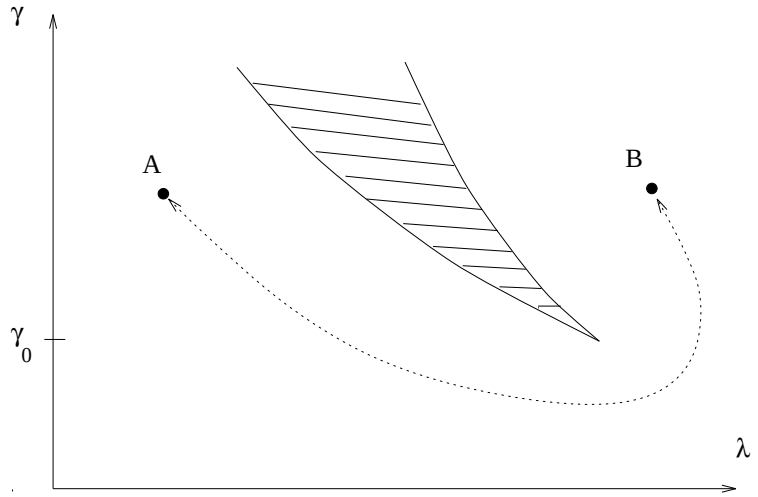

Fig. 16. Jump-free path (dotted) in the parameter plane.

ory of singularites has been established to analyze related higher-order bifurcations [Golubitsky & Schaeffer, 1985].

11. Other problems

The model problem in Eq.(1) is a representative of a huge class of applications. But there are other problems equally important, and not covered by Eq.(1). For example, many classical oscillation problems are non-autonomous, such as

$$\ddot{u} + f(u, \dot{u}) = \gamma \cos \omega t. \tag{10}$$

The transformation $y_1 := u$, $y_2 := \dot{u}$, $y_3 := t$ leads to a problem of type (1), but this transformation may not be always advisable. Another class of problems not immediately of the form in Eq.(1) are ODE boundary-value problems

$$\mathbf{y}' = \mathbf{f}(t, \mathbf{y}, \lambda), \quad \mathbf{r}(\mathbf{y}(a), \mathbf{y}(b)) = \mathbf{0}. \tag{11}$$

Problems of this type describe, for example, *Turing instabilities* that are a mechanism of one-dimensional pattern formation. The ODE situation discussed so far is a special case of PDEs. PDE models may exhibit ODE bifurcations and many further nonlinear phenomena. Both spatial and temporal phenomena need be studied. Reaction-diffusion problems of the type

$$\mathbf{y}_t = \mathbf{D}\nabla^2\mathbf{y} + \mathbf{f}(\mathbf{y}, \lambda) \tag{12}$$

comprise all ODE settings. For vanishing diffusion ($\mathbf{D} = \mathbf{0}$) the model problem of Eq.(1) results. On the other hand, for a stationary situation ($\dot{\mathbf{y}} = \mathbf{0}$, one space variable) the PDE (12) reduces to an ODE boundary-value problem of type (11). The former case models purely temporal dynamics of the reaction-diffusion problem, whereas the latter case concentrates on purely spatial patterns. In the general case, temporal and spatial phenomena may be interrelated in complicated ways.

12. Historical and bibliographical remarks

Early studies of nonlinearity include Euler's buckling problem [1744], and the work of Poincaré [1885]. Classical experimental studies were performed for fluid flow by Bénard [1901], and Taylor [1923]. Analytical investigations are numerous; we mention Liapunov's work on stability [1892], the studies of Andonov and coworkers on "Hopf bifurcation" in the 1930s [1987], Hopf's general theorem [1942], Rayleigh's analysis of convection [1916], and the book by Arnol'd on geometrical methods [1983]. Since the advent of powerful computers and algorithms the field has grown dramatically. The literature is rich, and here is not the space to present a survey. An elementary text book with many examples and practical hints is [Seydel, 1994]. Other texts are oriented more analytically. We mention a few examples, [Guckenheimer & Holmes, 1983], [Arrowsmith & Place, 1990], [Golubitsky & Schaeffer, 1985], [Chow & Hale, 1982], on Hopf bifurcation [Hassard *et al.*, 1981], and on the chaos-oriented side, [Devaney, 1986], [Marek & Schreiber, 1991], [Schuster, 1984].

References

Andronov, A.A., Vitt, A.A. & Khaikin, S.E. [1987] *Theory of Oscillators* (Dover Publications, New York).

Arnol'd, V.I. [1983] *Geometrical Methods in the Theory of Ordinary Differential Equations* (Springer, New York).

Arrowsmith, D.K. & Place, C.M. [1990] *An Introduction to Dynamical Systems* (Cambridge University Press, Cambridge).

Bénard, H. [1901] "Les tourbillons cellulaires dans une nappe liquide transportant de la chaleur par convection en regime permanent," *Ann. Chim. Phys.* **7**, Ser. 23, p. 62.

Chow, S.-N. & Hale, J.K. [1982] *Methods of Bifurcation Theory* (Springer, New York).

Devaney, R.L. [1986] *An Introduction to Chaotic Dynamical Systems* (Menlo Park, Benjamin).

Euler, L. [1744] "De Curvis Elasticis, Methodus Inveniendi Lineas Curvas Maximi Minimive Proprietate Gaudentes. Additamentum I. ," in *Opera Omnia I* Vol.24, 231–297, Zürich 1952.

Golubitsky, M. & Schaeffer, D.G. [1985] *Singularities and Groups in Bifurcation Theory. Vol.1* (Springer, New York).

Guckenheimer, J. & Holmes, Ph. [1983] *Nonlinear Oscillations, Dynamical Systems and Bifurcation of Vector Fields* (Springer, New York).

Hassard, B.D., Kazarinoff, N.D., Wan, Y.-H. [1981] "*Theory and Applications of Hopf Bifurcation* (Cambridge University Press).

Holodniok, M. & Kubíček, M. [1984] "DERPER—an algorithm for the continuation of periodic solutions in ordinary differential equations," *J. Comput. Phys.* **55**, 254–267.

Hopf, E. [1942] "Abzweigung einer periodischen Lösung von einer stationären Lösung eines Differentialsystems," (Bericht der Math.-Phys. Klasse der Sächsischen Akademie der Wissenschaften zu Leipzig 94).

Krug, H.-J. & Kuhnert, L. [1985] " Ein oszillierendes Modellsystem mit autokatalytischem Teilschritt," *Z. Phys. Chemie* **266**, 65–73.

Liapunov, A.M. [1892] *Stability of Motion* (Academic Press, New York, 1966).

Marek, M. & Schreiber, I. [1991] *Chaotic Behaviour of Deterministic Dissipative Systems.* Cambridge University Press

Poincaré, H. [1885] "Sur l'équilibre d'une masse fluide animée d'un mouvement de rotation," *Acta Mathematica* **7**, 259–380.

Pönisch, G. & Schwetlick, H. [1982] "Ein lokal überlinear konvergentes Verfahren zur Bestimmung von Rückkehrpunkten implizit definierter Raumkurven," *Numer. Math.* **38**, 455–465.

Lord Rayleigh [1916] "On convection currents in a horizontal layer of fluid, when the higher temperature is on the under side," *Philos. Mag.* **32**, 529–546.

Schuster, H.G. [1984] *Deterministic Chaos* (Physik-Verlag, Weinheim).

Seydel, R. [1994/2010] *Practical Bifurcation and Stability Analysis. From Equilibrium to Chaos. Second Edition. Springer Interdisciplinary Applied Mathematics, Vol.* **5**. (Springer, New York). Third Edition 2010.

Smith, C.B., Kuszta, B., Lyberatos, G. & Bailey, J.E. [1983] "Period doubling and complex dynamics in an isothermal chemical reaction system," *Chem. Eng. Sci.* **38**, 425–430.

Taylor, G.I. [1923] "Stability of a viscous liquid contained between two rotating cylinders," *Philos. Trans. Roy. Soc. London* **A 223**, 289–343.